MUC-NOTE-DECAY_CHANNEL-289
9 February 2004

Optimizing the Pion Capture and Decay Channel

K. Paul

Department of Physics
University of Illinois at Urbana-Champaign
1110 West Green Street
Urbana, IL 61801

C. Johnstone

Fermi National Accelerator Laboratory
Batavia, IL 60510

Abstract

The following study attempts to quantify a few tunable and easily understood parameters that determine the design and performance of the pion capture and decay channel in current US neutrino factory schemes. This study considers a variety of designs with various design parameters that describe the field strength profile in the channel and computes the muon yield at the end of the decay channel for each design using MARS. It is found that muon yields of as large as $Y_\mu = 0.53\ \mu/P$ are achievable with a carbon target. Crude cost considerations are made for the different designs, as well.

1 Introduction

With the completion of the second neutrino factory feasibility study (FS2) [1], and with the upcoming third feasibility study looming on the horizon (FS2a), some effort should be made to reanalyze the pion and muon collection scheme. The pion capture section proposed in the second feasibility study includes a 20 T solenoid surrounding the target, designed to capture pions with a transverse momentum less than 225 MeV/c in a beampipe with a radius of 7.5 cm surrounding a mercury jet target. The capture section is then followed (downstream) by a 18.62 m tapered solenoid, adiabatically taking the pions (and muon decay products) from the 20 T, 7.5 cm radius region at the target to a 1.25 T, 30 cm radius decay channel. The overall length of the capture and decay channel is 50 m, including a 3 m matching section between the downstream end of the decay channel and the upstream end of the buncher and phase-rotation system that follows.

Final optimization of the pion capture and decay channel requires a detailed knowledge of the upstream and downstream elements in the neutrino factory design, such as the apertures and momentum acceptances of the buncher/phase-rotation system and the cooling channel, as well as the beam energy and power of the chosen proton driver. These elements are, themselves, still in development, which means that the final word on the pion capture and decay channel has yet to be said. Ideally, the final optimization should be done simultaneously with all elements in the design, and work in this direction is being done.

However, there are still useful statements to be made regarding the optimizable properties of the capture and decay channel, if simply to fully understand its behavior. While the general properties of the capture and decay channel are well understood–namely, adiabaticity and pion decay–a continuum of design options still exist and have yet to be explored. Most of these options differ in the specific shape and strength of the field in the channel, all of which contribute to the overall cost and performance of the channel. This study is designed to explore a number different design schemes in an attempt to better understand the detailed principles involved in the generation of the muon beam and design a channel in terms of easily tunable, and understandable, parameters that can be determined at a later stage.

In the next section, Section 2, we discuss the general design of the capture and decay channel used in this study, for the most part reviewing the design proposed in the second feasibility study. The following section, Section 3, discusses the design of the tapered solenoids and the effects of adiabaticity on the total muon yields at the end of the decay section. Then, in Section 4, we expand on this design by considering increased magnetic field strength in the decay channel, studying the effects of the field strength on capturing the muons produced from pion decay. In the next section, Section 5, we comment on the method of fitting short current coils to the field strength profiles discussed in the prior sections, and in the final section, Section 6, we summarize the results, make what conclusions can be made, and comment on the direction of future work.

2 Channel Design

For the purposes of this study, we will assume a 1 MW incident beam of 16 GeV protons on an 80 cm carbon target, as discussed in the first neutrino factory feasibility study (FS1) [2]. There is no doubt that a mercury target will have significantly better charged pion yields, as would a more energetic incident proton beam. However, we have decided to be very conservative in this study, avoiding the inherent difficulties associated with the mercury jet target and opting for a 16 GeV beam in order to more easily compare results to prior findings, such as those in the first and second feasibility studies. In the end, the target section that we consider is essentially identical to that considered in FS1: an 80 cm long, 1.5 cm wide graphite target suspended in a 20 T solenoid at an angle of 50 mrad with respect to the central axis of the solenoid. The incident proton beam, therefore, enters at 50 mrad with respect to the central axis of the solenoid such that it travels along the central axis of the target.[1] No changes to this target design are

[1] The configuration chosen in FS1 actually considers a carbon target tilted at 50 mrad in order to place the pro-

considered, and only the elements of the capture and decay channel that are downstream from the target region are modified in this study.

The field strength of the capture solenoid, $B_0 = 20$ T, is chosen to contain charged pions with a transverse momentum of $p_T \leq 225$ MeV/c within a beampipe of radius $R_0 = 7.5$ cm. As one can see from Figure 1, this constitutes most of the charged pions produced from the carbon target. Then, by adiabatically decreasing the field strength while simultaneously increasing the radius of the beampipe such that the magnetic flux, $\Phi = \pi B R^2$, is conserved as one moves downstream from the target, the charged pion beam will increase in radius while decreasing in divergence. By demanding that the magnetic flux remain constant downstream of the target, the field strength at the end of the decay channel, where the beampipe has a radius of $R_f = 30$ cm to match into the buncher/phase-rotation system, will be

$$B_f = B_0 \left(\frac{R_0}{R_f}\right)^2 = 1.25 \text{ T} \ . \qquad (1)$$

Decreasing the field strength adiabatically means decreasing the magnetic field slowly such that the Larmor radius of the particles, $a = \frac{p_\perp}{eB}$ where $p_\perp$ is the magnitude of the momentum perpendicular to the magnetic field $\vec{B}$, satisfy the adiabatic constraints

$$a \ll R_B \ , \qquad (2)$$

where R_B is the radius of curvature of the magnetic lines of force, and

$$a \ll B \left(\frac{\partial B}{\partial s}\right)^{-1} \ , \qquad (3)$$

where s is the arc length measured along the central axis of the solenoids. It can be easily seen that these constraints are more difficult to satisfy in low-field regions where the Larmor radius, a, can be large.

Once the charged pions are transfered from the high field region into the low field region, a length of uniform solenoid is needed to contain the beam while the majority of charged pions decay into muons via their dominant decay mode, $\pi^+ \to \mu^+ \nu_\mu$ or $\pi^- \to \mu^- \bar{\nu}_\mu$, with a lifetime of $\tau_\pi \approx 26$ ns. The resulting muons will begin decay via their dominant decay mode, $\mu^+ \to e^+ \nu_e \bar{\nu}_\mu$ or $\mu^- \to e^- \bar{\nu}_e \nu_\mu$, with a much longer lifetime of $\tau_\mu \approx 2$ μs. A crude approximation of the necessary overall length of the channel can be made by assuming a monochromatic beam of N_0 charged pions produced from the target. Assuming no losses other than decay, the fraction of pions in the beam after a longitudinal distance s is traversed will be $f_\pi(s) = \exp -\frac{s}{c\tau_\pi}\frac{m_\pi c}{(p_\pi)_s}$, where the pions have longitudinal momentum $(p_\pi)_s$. Then, the fraction of muons in the beam will be

$$\begin{aligned} f_\mu(s) &= \left[1 - \exp\left(-\frac{s}{c\tau_\pi}\frac{m_\pi c}{(p_\pi)_s}\right)\right] \\ &\quad \times \exp\left(-\frac{s}{c\tau_\mu}\frac{m_\mu c}{(p_\mu)_s}\right) \ , \end{aligned} \qquad (4)$$

where we assume all of the muons are produced with roughly equal longitudinal momentum, $(p_\mu)_s$. The maximum of this function occurs at the distance

$$s_{max} = c\tau_\pi \left(\frac{(p_\pi)_s}{m_\pi c}\right) \ln\left[1 + \frac{(p_\mu)_s}{(p_\pi)_s}\frac{m_\pi}{m_\mu}\frac{\tau_\mu}{\tau_\pi}\right] \ . \qquad (5)$$

Based on the momentum distribution of pions produced from the target, shown in Figure 2, one can crudely approximate the longitudinal momentum of the pions and muons as $(p_\pi)_s \approx (p_\mu)_s \approx 250$ MeV/c, which results in an optimal channel length of $s_{max} \approx 65$ m. Throughout this study, we assume a 50 m overall channel length, after which 99%/97%/95% of the pions with longitudinal momenta 200/250/300 MeV/c have decayed.

At the end of the capture and decay channel, we expect a matching section to transfer the beam efficiently into the next stage in the design, such as the buncher and phase-rotation system. As already mentioned, current designs for the buncher and phase-rotation system incorporate a 1.25 T solenoid field. This means that if we match the 1.25 T field strength and the beampipe aperture at the beginning of the buncher and phase-rotation system to the end of the decay channel, no additional matching section should be required. If a different field strength is used in the decay channel, as will be

ton beam dump approximately 6 m downstream from the target. However, increasing the tilt angle 150 mrad provides approximately 30% greater than pion-muon yields.

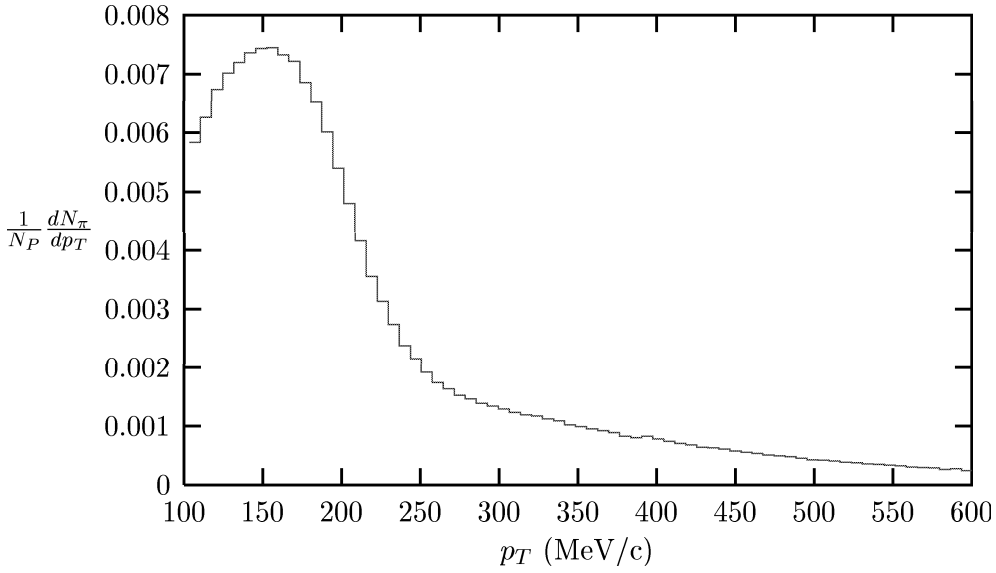

Figure 1: Transverse momentum distribution of the forward-going charged pions produced from an 80 cm carbon target with 16 GeV incident protons, divided by the total number of protons on target.

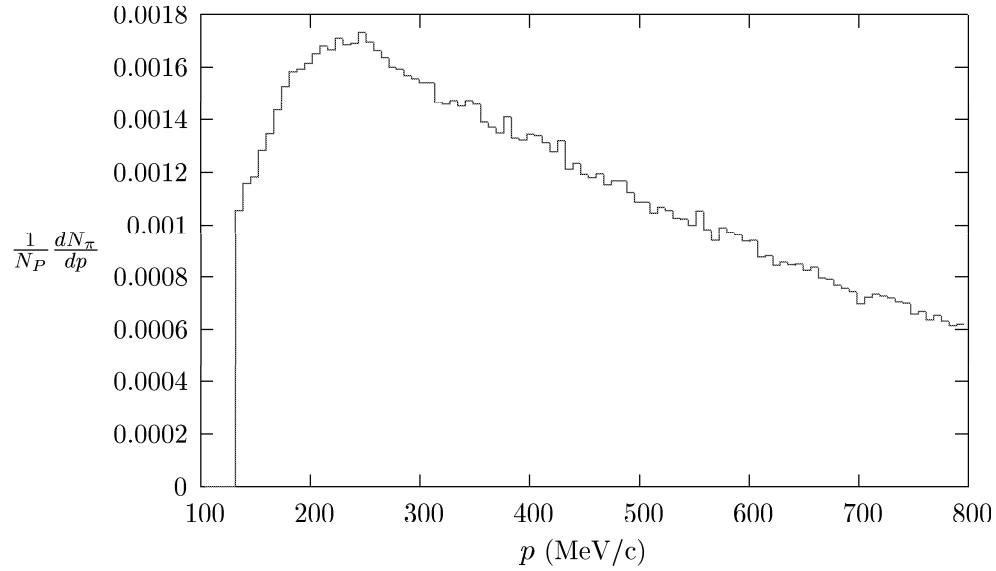

Figure 2: Momentum distribution of the forward-going charged pions produced from an 80 cm carbon target with 16 GeV incident protons, divided by the total number of protons on target.

discussed in Section 4, an additional matching section (tapered solenoid) must be added to take the beam from the field strength in the decay channel to the matched 1.25 T field strength.

For the purposes of clarity, we will from here out refer to the 20 T solenoid surrounding the target as the *capture solenoid*. The uniform, low-field solenoid that allows for the necessary 50 m of decay straight will be called the *decay solenoid*. The tapered solenoid that transfers the charged pions from the high-field capture solenoid into the low-field decay solenoid will be called the *primary matching section*, and if a matching section is required following the decay solenoid to take the beam into the buncher and phase-rotation system, this will be called the *secondary matching section*. While the individual lengths of each section may vary with the considered design, we will assume that the overall length of the channel is 50 m for all designs.

3 Adiabatic Matching Sections

As was already mentioned in the previous section, the matching sections are designed to be adiabatic, as defined by the conditions for adiabaticity given in Equations 2 and 3. If these conditions are met, then the motion of the particles in the adiabatically varying region can best be understood in terms of the adiabatic invariants Ba^2 and $\frac{p_\perp^2}{B}$ [3]. That is, as the beam travels downstream from the target, its divergence decreases. Simultaneously, since the Larmor radius of the particles, a, increases, the spot size of the beam must correspondingly increase.

To ensure that the conditions for adiabaticity are satisfied, we must design the matching sections to decrease the curvature and gradient as much as possible. To do this, we parametrize the beampipe radius as a function of arc length along the central axis of the channel, $R(s)$, in terms of a few design parameters that can be tuned to provide optimal performance (e.g., length of the matching section, initial and final beampipe radii, field shape parameters, etc.) while remaining simple enough for the physics of the design to be easily understood. This *radius function* effectively describes the trajectory of the outermost lines of force, the lines of force running parallel to the beampipe. It is these lines of force that have the largest curvature and are, therefore, the lines of force whose curvature we are attempting to minimize.[2] Once a parametrization for the radius function is devised, the on-axis field strength in the matching section can be computed from conservation of flux.

For the purposes of this section, let us consider a 1.25 T decay solenoid, such that the upstream and downstream end radii of the primary matching section are fixed due to conservation of magnetic flux through the beampipe,

$$R(s_1) \equiv R_1 = 7.5 \text{ cm} \ , \quad (6)$$

$$R(s_2) \equiv R_2 = 30 \text{ cm} \ , \quad (7)$$

where s_1 and s_2 are the arc length positions of the upstream and downstream ends of the matching section, respectively. The secondary matching section can be neglected since no matching is required to take the beam from the 1.25 T decay solenoid into the 1.25 T buncher/phase-rotation system. To remain general, we will leave s_1 undefined, and $s_2 - s_1$, the overall length of the matching section, will be one of the tunable parameters used to optimize the channel.

In addition to matching the strength of the field at the upstream and downstream ends of the solenoid, we will also consider two constraints on the radius function that match the direction of the lines of force at the upstream and downstream ends of the matching section. The designs in the first and second feasibility studies consider a divergence in the field at the upstream end of the matching section, even though such a design is impossible to reasonably fit with realistic fields. Thus, for the sake of comparison, we allow for the lines of force at the upstream end of the matching section to be divergent, meaning that the slope of the radius function at the upstream end can be non-zero,

$$\frac{\partial R}{\partial s}(s_1) = \lambda \ . \quad (8)$$

This slope parameter, λ, will be another tunable parameter used to optimize the channel, though only $\lambda = 0$ designs can be reasonably fit with

[2] It should be noted that the physical beampipe radius, $R_p(s)$, need not exactly match the beampipe radius function, $R(s)$, described above. The physical radius function need only satisfy the condition $R_p(s) \geq R(s)$.

realistic fields. More will be said on this in Section 5.

At the downstream end of the matching section, the lines of force should be parallel, so we demand that the slope of the downstream end of the radius function be zero,

$$\frac{\partial R}{\partial s}(s_2) = 0 \quad . \tag{9}$$

The choice for the radius function used in the second feasibility study was

$$R_{FS2}(s) = \sqrt{R_1^2 + (R_2^2 - R_1^2)\left(\frac{s - s_1}{s_2 - s_1}\right)} \quad , \tag{10}$$

defined over the range $s_1 \leq s \leq s_2$. With the upstream and downstream radii fixed by field strengths, this design has only one tunable parameter: the length of the matching section, $s_2 - s_1$. It does not match the direction of the magnetic field at the upstream ends, so it does not satisfy the constraints given by Equations 8 and 9.

In this study, we opt to define a more general general radius function,

$$R(s) = (\alpha_0 + \alpha_1 s + \alpha_2 s^2 + \alpha_3 s^3)^{\frac{1}{k}} \quad , \tag{11}$$

defined over the range $s_1 \leq s \leq s_2$. Using the four constraints given above, we can solve for the polynomial parameters $\alpha_i(R_1, R_2, s_1, s_2, \lambda, k)$. Then, we can separately study the performance of the channel for various values of k, λ, and $s_2 - s_1$. For the second feasibility study, $s_1 = 0$ m, $s_2 = 18.62$ m, $k = 2$,

$$\begin{aligned} \alpha_0 &= R_1^2 - (R_2^2 - R_1^2)\frac{s_1}{s_2 - s_1} = 56.25 \text{ cm}^2 \quad , \\ \alpha_1 &= (R_2^2 - R_1^2)\frac{1}{s_2 - s_1} = 0.4531 \text{ cm} \quad , \end{aligned}$$

$\alpha_2 = 0$, and $\alpha_3 = 0$ cm^{-1}.

To study the effects of adiabaticity on the performance of the channel, full simulations of the target region, matching sections, and decay solenoid were done using MARS [4]. Hence, pion production and decay, as well as transport of the beam to the end of the decay channel (50 m downstream from the target), were all done in the same code. The muon yield, $Y_\mu = Y_{\mu^+} + Y_{\mu^-}$, at the end of the decay channel was computed for a wide range of design parameters: $s_2 = 250, 500, 1000, 2000$ cm, $0 \leq \lambda \leq 0.30$, and $k = 1, 2$. For all of the designs considered in this section it is assumed that $R_1 = 7.5$ cm, $R_2 = 30$ cm, and $s_1 = 0$ m.

Given a choice of parameters defining the channel, the on-axis magnetic field down the center of the channel is assumed to be

$$B(s) = B_1 \left(\frac{R_1}{R(s)}\right)^2 \quad , \tag{12}$$

where $B_1 = 20$ T and $R_1 = 7.5$ cm. Then, the magnetic field is computed using an off-axis expansion in the distance from the central axis, assuming cylindrical symmetry. This *ideal* field is used for the numerous MARS simulations made in this study, and these runs should be thought of as an attempt to find the preferred on-axis field strength profile to which we will then fit a long series of short current coils.

Figure 3 shows the muon yields from MARS simulations for a variety of design parameters, plotted as functions of the slope parameter, λ. As on can see from the figure, the longer matching sections result in larger yields, as one might have guessed since longer matching sections naturally have smaller curvature and normalized field gradient. It is also interesting to note that the optimal yield, for a given length matching section, seems independent of the choice of $k = 1, 2$. However, the dependence of the yield on the initial slope parameter, λ, is dramatic and becomes more dramatic as the length of the matching sections are increased. Most importantly, since the $\lambda = 0$ designs are the only designs that can be realistically fit, one should observe that the longer matching section designs appear to prefer smaller λ.

While yield is significantly important to the physics potential of the design, cost is important to its feasibility. With this in mind, we must consider the overall cost of the capture and decay channel as well as its performance. The cost of the channel is roughly proportional to the energy stored in the magnetic field of the solenoids. To consider both cost and performance simultaneously, we construct a merit factor equal to

$$f \equiv \frac{Y_\mu}{W} \quad , \tag{13}$$

where Y_μ is the muon yield of the channel (μ/P) and W is the energy stored in the channel's

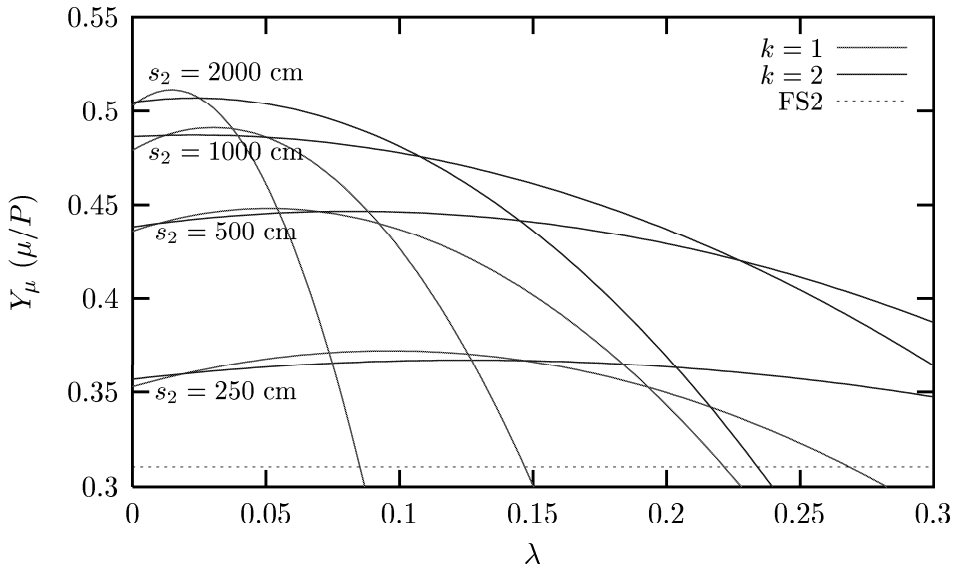

Figure 3: Muon yields at the end of the 1.25 T decay solenoid for designs with various matching section parameters: $R_1 = 7.5$ cm, $R_2 = 30$ cm, $s_1 = 0$ m, $s_2 = 250, 500, 1000, 2000$ cm, and $k = 1, 2$. The yields are shown as functions of the slope parameter, λ, with the largest yields coming from the designs with longer matching sections. The single data point shows the yield expected from the design considered in the second feasibility study.

magnetic field. For purposes of comparison, $Y_{FS2} = 0.311\ \mu/P^3$ is the yield of the FS2 channel and $W_{FS2} \approx 15$ MJ is the energy stored in the FS2 magnetic field.[4] Therefore, the FS2 channel would have a merit factor of $f_{FS2} = 0.033\ \mu/P$ MJ^{-1}.

Figure 4 shows the merit factors for each of the designs considered above, normalized to the merit factor of the design considered in the second feasibility study. Values in the figure above unity describe a design with an improved performance-to-cost ratio over the design suggested in the second feasibility study. The first thing that can be observed by the curves shown in the figure is that the normalized merit factor peaks at larger values of the slope parameter, λ, than does the yield. This comes from the fact that smaller slopes result in a longer high-field region at the upstream end of the primary matching section, or, alternately, larger slope parameters mean higher field gradients, resulting in a more rapid decrease in the field strength immediately following the target. A similar argument applies to the length of the primary matching section. A longer matching section has a smaller field gradient, resulting in a longer high-field region near the target. We can see this effect in the figure as well, noting that the $k = 2$, $s_2 = 500, 1000, 2000$ cm designs all have similar peak merit factors, though the $s_2 = 1000$ cm design appears to have the largest. The reader should keep in mind, though, that these merit factors are only meaningful if very good fits to the design can be made with realistic fields, and we will reiterate this in Section 5.

[3]This number is obtained by taking the quoted pion-plus-muon yields in the second feasibility study for a 16 GeV proton beam on a mercury target and dividing by a factor of 1.9 to compensate for the carbon target considered in this study.

[4]Only the field inside the beampipe is considered.

4 Field Strength

As the pions decay, the resulting muons continue down a trajectory similar to that of their parent pions, though not exactly the same. On average, the muon will be given a small momentum kick perpendicular to the pion's initial momentum. In the center-of-mass frame of the pion, the momentum of the muon will be

$$p = \frac{1}{2}\, m_\pi \left(1 - \frac{m_\mu^2}{m_\pi^2}\right) \quad , \tag{14}$$

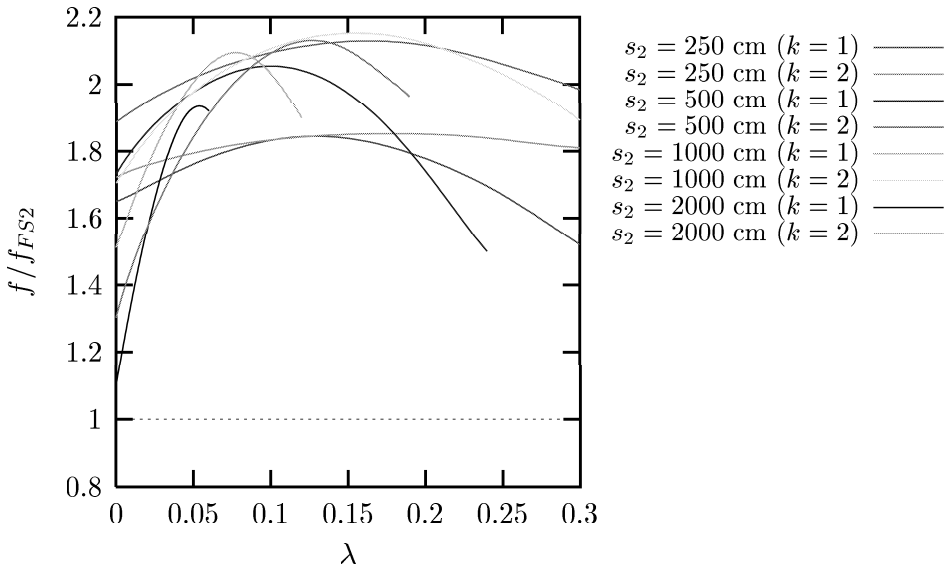

Figure 4: Normalized merit factors for the 1.25 T decay solenoid design with various matching section parameters: $R_1 = 7.5$ cm, $R_2 = 30$ cm, $s_1 = 0$ m, $s_2 = 250, 500, 1000, 2000$ cm, and $k = 1, 2$. The merit factor for each design is normalized to the merit factor of the second feasibility study design such that values above unity describe an improved performance-to-cost ratio. The designs considered in this figure are equivalent to the designs considered in Figure 3.

and in the pion center-of-mass frame, the muon's emission will be uniformly distributed in all directions since the pion has no spin. In the pion center-of-mass frame, the component of the muon's momentum perpendicular to the direction of the pion in the lab frame will be

$$p_\perp = \frac{1}{2}\, m_\pi \left(1 - \frac{m_\mu^2}{m_\pi^2}\right) \sin\theta_{CM} \quad , \qquad (15)$$

where θ_{CM} is the angle between the muon momentum in the center-of-mass frame and the direction of the pion in the lab frame. Boosting into the lab frame leaves the perpendicular component invariant. Averaged over all directions in the center-of-mass frame, we find the average component of the muon perpendicular to the pion momentum in the lab frame to be

$$\langle p_\perp \rangle = \frac{1}{4}\, m_\pi \left(1 - \frac{m_\mu^2}{m_\pi^2}\right) \approx 15 \text{ MeV/c} \quad . \qquad (16)$$

In an ideal case, the pions will be close to the central axis of the beampipe with zero transverse momentum, meaning that the muons will receive an average transverse momentum kick from pion decay equal to $\langle p_T \rangle \approx \langle p_\perp \rangle \approx 15$ MeV/c.

In a $B = 1.25$ T decay solenoid with a beampipe radius of $R = 30$ cm, the largest transverse momentum that a particle can have and remain contained by the solenoidal field is given by

$$p_T \leq e\, B \left(\frac{R}{2}\right) \approx 56 \text{ MeV/c} \quad , \qquad (17)$$

assuming the particle starts near the central axis of the beampipe. This is less than four times the average transverse kick given to a muon resulting from pion decay, and many of the parent pions will decay off of the central axis with non-zero transverse momentums of their own. Hence, it is reasonable to assume that a noticeable fraction of the produced muons will be given a large enough transverse momentum kick from pion decay to eject them from the beampipe.

To compensate for this, one must observe that the average transverse momentum kick given to a muon due to pion decay is independent of the field strength in the channel. Hence, one might hope to hold on to more muons by increasing the field strength in the decay channel. With this in mind, we reproduced the designs considered in the previous section with a 2.00 T and 3.00 T decay solenoid. In these designs, we still assume that the channel must be matched into a 1.25 T buncher and phase-rotation system, so the last 10 m of the decay channel is replaced with a sec-

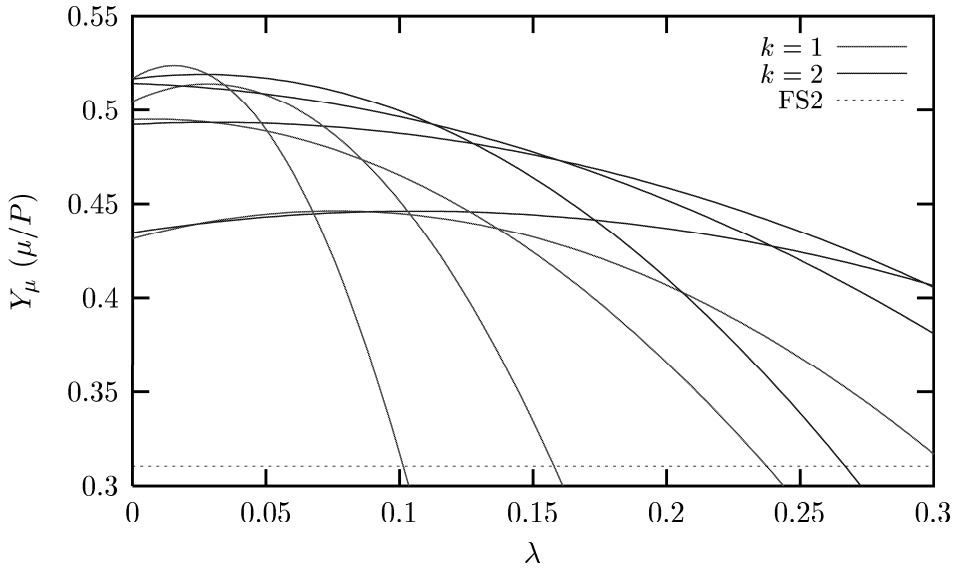

Figure 5: Muon yields at the end of the 2.00 T decay solenoid for designs with various matching section parameters: $R_1 = 7.5$ cm, $R_2 = 30$ cm, $s_1 = 0$ m, $s_2 = 250, 500, 1000, 2000$ cm, and $k = 1, 2$. The yields are shown as functions of the slope parameter, λ, with the largest yields coming from the designs with longer matching sections. The single data point shows the yield expected from a 2.00 T decay channel design based on the design considered in the second feasibility study.

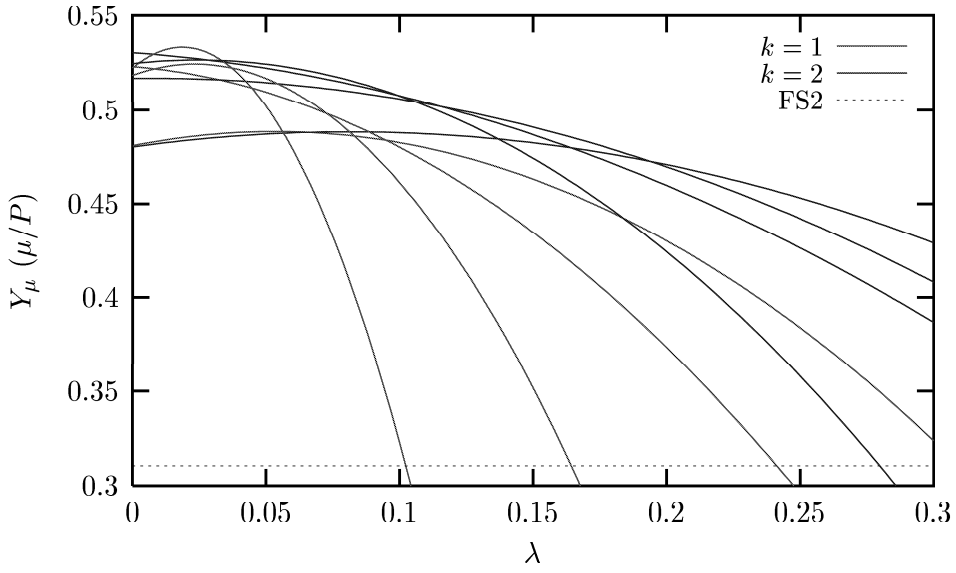

Figure 6: Muon yields at the end of the 3.00 T decay solenoid for designs with various matching section parameters: $R_1 = 7.5$ cm, $R_2 = 30$ cm, $s_1 = 0$ m, $s_2 = 250, 500, 1000, 2000$ cm, and $k = 1, 2$. The yields are shown as functions of the slope parameter, λ, with the largest yields coming from the designs with longer matching sections. The single data point shows the yield expected from a 3.00 T decay channel design based on the design considered in the second feasibility study.

ondary matching section taking the beam from the field in the decay channel to the 1.25 T field required.[5] The overall length of the capture and decay channel, therefore, is still 50 m.

The yields for the 2.00 T decay solenoid designs are shown in Figure 5 for various design parameters. Again, for reference, we note the quoted yields from second feasibility study. The results are similar to the results found in the case with the 1.25 T decay solenoid. The yield of the shorter matching section designs ($s_2 = 250, 500$ cm) improve significantly in the higher field, but the long matching section designs ($s_2 = 1000, 2000$ cm) have optimal yields only a few percent greater than the lower field designs.

The yields for the 3.00 T decay channel designs are shown in Figure 6 for various design parameters. Again, the results are similar, showing a significant increase in yields for shorter matching section designs, and little increase in optimal yields for the long matching section designs.

Increasing the strength of the field, however, increases the cost of the channel. So, we must also consider the merit factors of the higher-field designs. The normalized merit factors for the 2.00 T and 3.00 T decay channel designs are shown in Figures 7 and 8, respectively. These figures suggest that the slight performance increase provided by an increased field decay channel is not enough to compensate the increased cost since the data suggests an overall decrease in the normalized merit factor as the field strength in the decay solenoid increases.

5 Realistic Fields

The data accumulated for this study was done using non-Maxwellian fields. Namely, the field in the beampipe is computed using an off-axis expansion from the *ideal* on-axis field strength profile computed from a radius function, $R(s)$, with a discontinuity at $s = s_1$. This naturally raises the question of the validity of the simulations and of the numbers quoted in the previous sections. Thus, some discussion of fitting to the on-axis field strength profile should be given.

[5]The secondary matching section, in all cases, has design parameters $k = 1$ and $\lambda = 0$.

For small slope parameters designs, $\lambda \sim 0$, a Maxwellian fit to the on-axis field strength, $B(s)$, can be made without difficulty. For the specific case of zero slope, the on-axis field, $B(s)$, has no discontinuity in its derivative, and the field produced from the off-axis expansion is almost identical to that found from a fitted series of short current coils, assuming the inner radius of the coils is slightly larger than the beampipe radius itself.

As the value of the slope parameter increases, it becomes increasingly difficult to find an accurate fit to the ideal on-axis field strength profile, $B(s)$. At some point, one must compromise the idealized uniform field at in the target region. This presents some new problems because the design of the target, which was not altered in this study, was chosen assuming a uniform 20 T field in the target region. Thus, by changing the field in the target region, one runs the risk of producing fewer pions from the target, and based on runs made with a number of different fits to profiles found in this study, the decrease in pion yield from the target can be dramatic depending on the shape of the field in the target region. In fact, realistic fits to some of the high-λ designs suggested an inherent danger in creating "spikes" in the target-region field. Such sudden increased in the field near the target can act as a magnetic mirror for high-p_T pions produced at the upstream end of the target. This results in fewer pions being transfered into the decay channel.

For the most part, the ability to accurately reproduce the yields quoted in this study with realistic magnetic fields depends on the configuration of current coils. The number of independent parameters available in such a designs is enormous, including the length, inner and outer radii, current density, and spacing between each coil. This makes finding a realistic fit to the ideal on-axis field strength a challenge for high-λ designs, and it was considered beyond the scope of this study.

With these disclaimers made, it should be said that the $Y_\mu = 0.53$ μ/P muon yield quoted for the optimal performance design has been reproduced with realistic fields. Realistic fields have been found for the designs with higher slope parameter, but in all cases the muon yields were

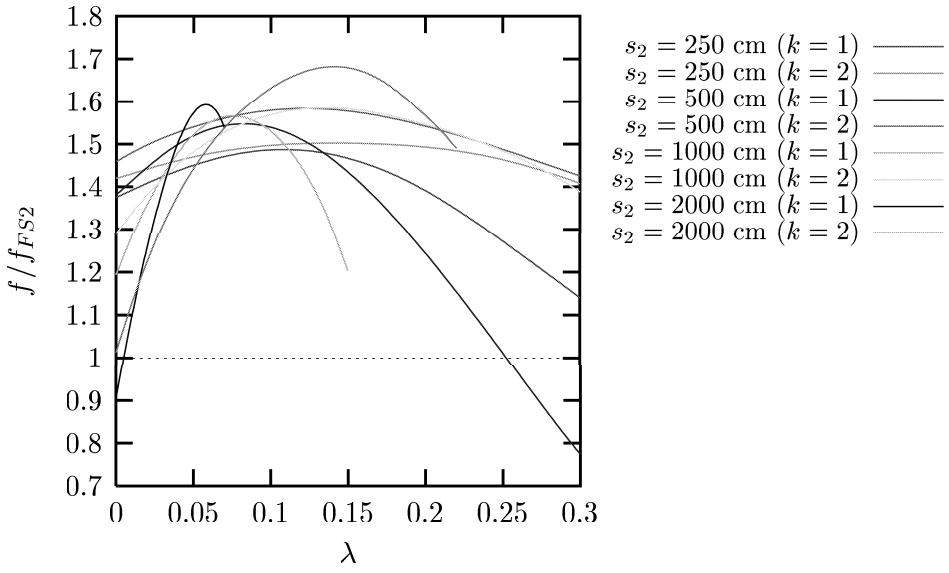

Figure 7: Normalized merit factors for the 2.00 T decay solenoid design with various matching section parameters: $R_1 = 7.5$ cm, $R_2 = 30$ cm, $s_1 = 0$ m, $s_2 = 250, 500, 1000, 2000$ cm, and $k = 1, 2$. The merit factor for each design is normalized to the merit factor of the second feasibility study design such that values above unity describe an improved performance-to-cost ratio. The designs considered in this figure are equivalent to the designs considered in Figure 5.

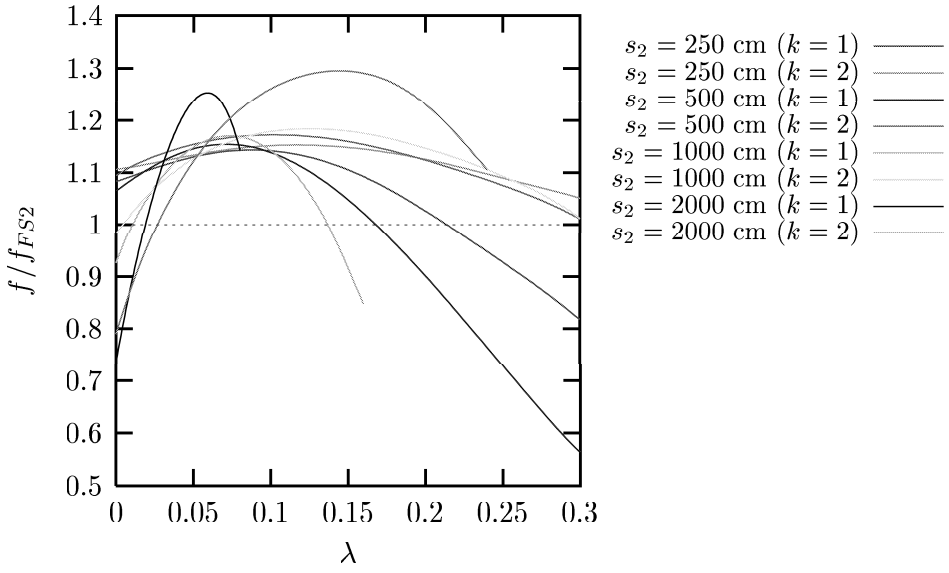

Figure 8: Normalized merit factors for the 3.00 T decay solenoid design with various matching section parameters: $R_1 = 7.5$ cm, $R_2 = 30$ cm, $s_1 = 0$ m, $s_2 = 250, 500, 1000, 2000$ cm, and $k = 1, 2$. The merit factor for each design is normalized to the merit factor of the second feasibility study design such that values above unity describe an improved performance-to-cost ratio. The designs considered in this figure are equivalent to the designs considered in Figure 6.

found to be significantly less than the ideal design. However, better fits could possibly have been made, so no definite conclusions are drawn from these results.

6 Conclusions

Making a final decision on the design parameters of the pion capture and decay channel is difficult at this stage. Final decisions on the energy of the proton beam and the design and material of the target need to be made before final numbers can be quoted on the expected muon yield. However, based on the MARS simulations done for this study, it appears that to achieve maximum muon yield reasonable designs consist of a relatively long primary matching section (20 m) with a relatively high magnetic field in the decay solenoid (2.00 T). Matching sections much longer than those considered in this study are impossible without making the channel, itself, longer, and many already believe that 2.00 T is the highest field that the decay channel can reasonably attain. From the MARS simulations done for this study, it appears that with these choices one can easily attain muon yields near $Y_\mu = 0.53\ \mu/P$, and this has been verified with realistic fields.

Assuming that the cost of the channel is proportional to the energy stored in the solenoidal magnetic field, one can compute a crude performance-to-cost ratio for a particular design. Based on these combined physics-financial considerations, it appears that the optimal capture and decay channel would have a 1.25 T decay solenoid with only a moderate-to-long length primary matching section (10-20 m). In these optimal performance-to-cost designs, the muon yields can be expected to be near $Y_\mu = 0.45-0.48$ μ/P, assuming a good fit to the ideal on-axis field strength can be made. While the yield is not as large as the purely physics-based optimal yields, the overall cost of the channel can be reduced by approximately 30%. This may save a few million dollars, but considering the overall cost of the neutrino factory and the difficulty in finding realistic field fits to such a high-λ design, it may be more cost effective overall to choose the high performance design described above.

One might also imagine simulating longer channels, allowing more time for the remaining pions in the channel to decay, as was suggested in Section 2. This will increase the cost of the channel proportionally, but for the same reasons given above, this may not be a problem. However, assuming a good match can be made into the subsequent buncher and phase-rotation system, many of the undecayed pions may remain in the beam, and their muon contribution to the beam may not be lost, thus eliminating the need for a longer channel.

This is just one of many reasons to optimize the capture and decay channel simultaneously with the buncher and phase-rotation system. With MARS, this would require a cumbersome and tedious joining of the MARS simulations to the ICOOL simulations in which the majority of the rest of the neutrino factory design has been implemented. Ideally, one would simulate the pion production, capture and decay in the same environment as the rest of the design. With that in mind, future work on this subject will be done in GEANT4, first reproducing the MARS simulations of the front-end devices, and then adding downstream elements in a piece-wise fashion.

References

[1] S. Ozaki *et al.*, BNL-52623.

[2] N. Holtkamp *et al.*, SLAC-REPRINT-2000-054.

[3] J.D. Jackson. *Classical Electrodynamics, 2nd Ed.* John Wiley & Sons, Inc. New York-London, 1975.

[4] N.V. Mokhov, "The Mars Code System User's Guide", Fermilab-FN-628 (1995). O.E. Krivosheev, N.V. Mokhov, "MARS Code Status", Proc. Monte Carlo 2000 Conf., p. 943, Lisbon, October 23-26, 2000; Fermilab-Conf-00/181 (2000); N.V. Mokhov, "Status of MARS Code", Fermilab-Conf-03/053 (2003); http://www-ap.fnal.gov/MARS/.